Title

Effect of Lithium-Ion Concentration on Morphology and Ion Transport in Single-Ion-Conducting Block Copolymer Electrolytes

Authors

Rojas, Adriana A
Inceoglu, Sebnem
Mackay, Nikolaus G
et al.

Effect of Lithium-Ion Concentration on Morphology and Ion Transport in Single-Ion-Conducting Block Copolymer Electrolytes

Adriana A. Rojas,[†,‡] Sebnem Inceoglu,[‡] Nikolaus G. Mackay,[†] Jacob L. Thelen,[†,‡] Didier Devaux,[‡,||] Gregory M. Stone,[⊥] and Nitash P. Balsara*[,†,‡,§,||]

[†]Department of Chemical and Biomolecular Engineering, University of California, Berkeley, Berkeley, California 94720, United States
[‡]Joint Center for Energy Storage Research (JCESR), [§]Materials Sciences Division, and [||]Environmental Energy Technologies Division, Lawrence Berkeley National Laboratory, Berkeley, California 94720, United States
[⊥]Malvern Instruments Inc., 117 Flanders Road, Westborough, Massachusetts 01581, United States

S *Supporting Information*

ABSTRACT: Single-ion-conducting polymers are ideal electrolytes for rechargeable lithium batteries as they eliminate salt concentration gradients and concomitant concentration overpotentials during battery cycling. Here we study the ionic conductivity and morphology of poly(ethylene oxide)-*b*-poly(styrenesulfonyllithium(trifluoromethylsulfonyl)imide) (PEO-*b*-PSLiTFSI) block copolymers with no added salt using ac impedance spectroscopy and small-angle X-ray scattering. The PEO molecular weight was held fixed at 5.0 kg mol^{-1}, and that of PSLiTFSI was varied from 2.0 to 7.5 kg mol^{-1}. The lithium ion concentration and block copolymer composition are intimately coupled in this system. At low temperatures, copolymers with PSLiTFSI block molecular weights ≤4.0 kg mol^{-1} exhibited microphase separation with crystalline PEO-rich microphases and lithium ions trapped in the form of ionic clusters in the glassy PSLiTFSI-rich microphases. At temperatures above the melting temperature of the PEO microphase, the lithium ions were released from the clusters, and a homogeneous disordered morphology was obtained. The ionic conductivity increased abruptly by several orders of magnitude at this transition. Block copolymers with PSLiTFSI block molecular weights ≥5.4 kg mol^{-1} were disordered at all temperatures, and the ionic conductivity was a smooth function of temperature. The transference numbers of these copolymers varied from 0.87 to 0.99. The relationship between ion transport and molecular structure in single-ion-conducting block copolymer electrolytes is qualitatively different from the well-studied case of block copolymers with added salt.
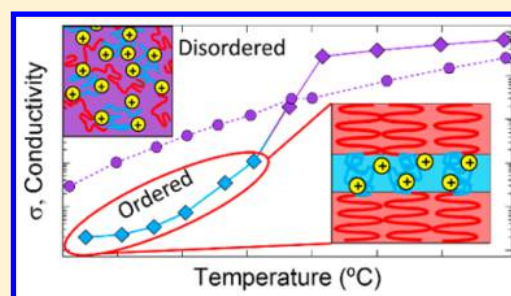
INTRODUCTION

There is continuing interest in electrolytes that are stable against lithium metal anodes.[1−3] Dry polymer electrolytes are more electrochemically and thermally stable when compared to conventional liquid electrolytes for lithium batteries. Most battery electrolytes are mixtures comprising a salt dissolved in a solvent. The salt dissociates into two (or more) ionic species, and the concentration gradients obtained during battery operation depend on the relative mobilities of the dissociated species. The resulting concentration overpotential is one of the factors that limit the rate at which batteries can be cycled.[4] Large salt concentration gradients can result in precipitation of the salt. Lithium dendrite growth rates are also dependent on the magnitude of the concentration gradients.[5] Polymer electrolytes wherein the anion is covalently bonded to the polymer backbone are of considerable interest because lithium ion transport in these systems occurs in the absence of concentration gradients.[6]

Bouchet and co-workers have synthesized and characterized a novel single-ion-conducting BAB triblock copolymer, polystyrene-*b*-poly(ethylene oxide)-*b*-polystyrene (SEOS), wherein lithium bis(trifluoromethane)sulfonylimide (LiTFSI) was co-

valently bonded to the styrene moieties in the polystyrene blocks.[7] Only the Li$^+$ is mobile because the TFSI$^-$ anion is covalently bonded to the glassy polystyrene (PS) backbone. However, PS is an ionic insulator while PEO is an ionic conductor. Thus, the Li$^+$ must be located in the PEO-rich microphase for efficacious ion transport.[3,8] There is practical interest in these electrolytes because ionic conductivities as high as 3.4 × 10^{-5} S cm^{-1} have been reported at 90 °C. Little is known about the morphology of this class of block copolymers. In contrast, extensive studies have been conducted on the relationship between conductivity and morphology in block copolymer binary electrolytes, i.e., block copolymers with added salt. An example of such a system is polystyrene-*b*-poly(ethylene oxide) (SEO)/LiTFSI wherein the salt is preferentially located in the PEO-rich microphase. These systems are known to microphase separate into ordered morphologies that enable independent control over mechanical and electrical properties, and increasing salt concentration

generally enhances the propensity for microphase separation.[3,9−16]

The objective of our study is to explore the dependence of ionic conductivity and cation transference number on morphology in a series of single-ion-conducting poly(ethylene oxide)-*b*-poly(styrenesulfonyllithium(trifluoromethyl sulfonyl)-imide) (PEO-*b*-PSLiTFSI) diblock copolymers (Figure 1). The
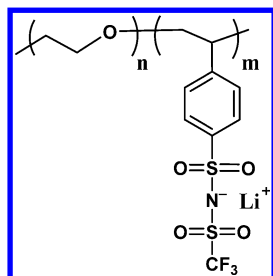

Figure 1. Chemical structure of PEO-*b*-PSLiTFSI. End groups are not shown.

molecular weight of the PEO block was held fixed at 5.0 kg mol^{-1} while the PSLiTFSI block molecular weight was varied from 2.0 to 7.5 kg mol^{-1}. The present paper builds upon work published in a Letter wherein results of a particular molecular weight of PEO-*b*-PSLiTFSI copolymer were described.[17]

■ EXPERIMENTAL SECTION

Polymers. PEO-*b*-PSLiTFSI diblock copolymers were synthesized and characterized as described in ref 17. The polymers were dialyzed with deionized water (4 L of water per gram of polymer) for 3 days to remove residual ionic impurities. Table 1 shows the samples that were used in this study. Polymers are labeled PEO−PSLiTFSI(*x*-*y*), where *x* and *y* are the nominal molecular weights of the PEO and PSLiTFSI blocks, respectively, in kg mol^{-1}. These copolymers were characterized by a Malvern Viscotek TDA 305 gel permeation chromatography (GPC) system with a mobile phase composed of 30 wt % acetonitrile and 70 wt % water containing 0.05 wt % of Na$_2$HPO$_4$ at a flow rate of 0.5 mL min^{-1}.[17] The GPC traces of the polymers, shown in Figure S1 (Supporting Information), confirm polymerization of the PSLiTFSI block. The PEO precursor sample contained a small high molecular weight shoulder. All of the block copolymer samples were approximately unimodal except for PEO−PSLiTFSI(5-2), which exhibited three GPC peaks: a main high-molecular-weight peak corresponding to the block copolymer and two additional peaks due to the unreacted PEO. We attribute this to the low concentration of the TFSI-containing monomer during polymerization.

The concentration of lithium ions increases with increasing molecular weight of the PSLiTFSI block. We quantify this concentration by *r*, defined as the molar ratio of lithium ions to ethylene oxide moieties, $r = [\text{Li}^+][\text{EO}]^{-1}$, without accounting for the end groups on either side of the chain. The volume fraction of the

PEO block (ϕ_{PEO}) is listed in Table 1, and it was estimated from the densities of PSLiTFSI homopolymer (1.57 g cm^{-3}) and PEO homopolymer (1.20 g cm^{-3}).[18] The density of the PSLiTFSI homopolymer was estimated using Van Krevelen's group contribution method, and the details of this calculation are shown in Table S1.[19] In addition to the polymers listed in Table 1, we also synthesized PEO-*b*-PSLiTFSI with PSLiTFSI molecular weights 10.2 and 10.6 kg mol^{-1}. These samples were brittle, and we were unable to make films necessary for conductivity measurements. We do not discuss these samples in this paper.

PEO-*b*-PSLiTFSI Sample Preparation. Polymer films for conductivity, transference number, and X-ray scattering were made by drop-casting from a 10 wt % solution in purified water obtained from a Barnstead NANOpure Diamond instrument (resistivity of 18.2 MΩ cm). Samples were allowed to dry in the fume hood for 12 h before they were brought into a vacuum oven at 45 °C, wherein they were allowed to dry for another 12 h. Thereafter, the samples were brought into an argon glovebox antechamber to dry under vacuum at 45 °C for 12 h before they were brought into the glovebox. Glove box integrity was maintained throughout subsequent sample preparation.

Electrochemical Impedance Spectroscopy. Each polymer film for electrochemical testing was placed in a Kapton spacer and melt-pressed in a custom-made hand-press at about 55 °C. Typical sample thicknesses ranged from 50 to 100 μm. Aluminum electrodes (18 μm in thickness) and aluminum tabs were used in the conductivity sample construction, and Kapton tape was used to seal the gap between the spacer and the electrode (see Figure S2 for a schematic of the cell). The conductivity samples were vacuum-sealed in pouch material (Showa-Denka), which allowed us to conduct electrochemical tests outside of the glovebox using a Bio-Logic VMP3 (variable multi-channel potentiostat). Ionic conductivity was determined from impedance spectroscopy measurements where a sinusoidal voltage of 50 mV was applied from 1 MHz to 1 Hz. The resistance was taken at the plateau value in the Bode plot of the modulus of the complex impedance, $|Z' + iZ''|$ vs ω (frequency). This value was identical to the resistance determined from the low-frequency minimum on a Nyquist impedance plot. Samples were placed in a custom-made heating stage, and they were studied at selected temperatures: from 25 to 60 °C in 5 deg increments and from 60 to 90 °C in 10 deg increments. Samples were then cooled down using the same temperature steps and subjected to a second heating cycle. The samples had an equilibration time of 15 min at each temperature. The reported conductivity values are from the second heating run. After the conductivity measurements were completed, the samples were carefully disassembled, and the thicknesses were measured with a micrometer. We report average ionic conductivities and standard deviations obtained using three independent samples.

Transference Number Measurement. The lithium/polymer/lithium symmetric cells used in the transference number measurements were similar to those described in the preceding paragraph, except that lithium electrodes were used instead of aluminum electrodes. Nickel tabs and nickel current collectors were used to complete the symmetric cell construction. These cells were also vacuum-sealed in pouch material. The steady-state current method was utilized, where chronoamperometry experiments were carried out on

Table 1. Characteristics of the Single-Ion-Conducting Block Copolymers Used in This Study[a]

sample	M_{PEO} (kg mol^{-1})	M_{PSLiTFSI} (kg mol^{-1})	Đ	$r = [\text{Li}^+][\text{EO}]^{-1}$	ϕ_{PEO}	t^+	d (nm)
PEO(5)	5.0	0	1.05	0	1	0	17.1
PEO−PSLiTFSI(5-2)	5.0	2.0	1.53	0.056	0.77	0.87	20.4
PEO−PSLiTFSI(5-3)	5.0	3.2	1.29	0.088	0.69	0.95	27.6
PEO−PSLiTFSI(5-4)	5.0	4.0	1.26	0.111	0.64	0.97	27.8
PEO−PSLiTFSI(5-5)	5.0	5.4	1.21	0.150	0.53	0.98	
PEO−PSLiTFSI(5-7)	5.0	7.2	1.25	0.199	0.49	0.99	
PEO−PSLiTFSI(5-8)	5.0	7.5	1.18	0.207	0.48	0.98	

[a]M_{PEO} = molecular weight of the PEO block; M_{PSLiTFSI} = molecular weight of the PSLiTFSI block; Đ = the dispersity; ϕ_{PEO} = volume fraction of the PEO block; t^+ = the lithium ion transference number; d = the domain spacing.

these cells at 90 °C using the VMP3 potentiostat.[20,21] A constant 20 mV potential was applied, and the current was measured as a function of time. Impedance spectra were collected at every hour increment to probe the bulk and interfacial resistances. These values were determined by fitting an equivalent circuit (Figure S4) to the data using EC-Lab and using eq S1 (see Supporting Information).

Small- and Wide-Angle X-ray Scattering (SAXS and WAXS). Measurements were made at beamline 7.3.3 at the Advanced Light Source at the Lawrence Berkeley National Laboratory (LBNL).[22] Silver behenate was used as a standard, and scattering patterns were reduced using the Nika program for IGOR Pro available from Jan Ilavsky at Argonne National Laboratories.[23] The background scattering from Kapton was subtracted from the reduced SAXS data. The azimuthally averaged scattering intensity, I, is reported as a function of the magnitude of the scattering vector, q. Polymer films for X-ray scattering were sealed in custom-made sample holders. Sample thicknesses ranged from 200 to 400 μm. Samples were placed in a custom-made heating stage, and they were studied using the same thermal history described in the Electrochemical Impedance Spectroscopy section. We report data obtained during the second heating cycle. We also conducted *in situ* experiments wherein SAXS and conductivity measurements were made simultaneously for the same samples for PEO—PSLiTFSI(5-2), -(5-3), -(5-4), and -(5-5). The data obtained from these measurements were consistent with the conductivity values reported herein.

Differential Scanning Calorimetry. Samples were hermetically sealed in aluminum pans in an argon glovebox. Differential scanning calorimetry (DSC) experiments were run with two heating and cooling cycles with 10 °C min^{-1} heating rates and 2 °C min^{-1} cooling rates using a Thermal Advantage Q200 calorimeter at the Molecular Foundry, LBNL. The temperature ranged from −90 to 150 °C. Melting and glass transition temperatures were obtained from analysis of the second heating run.

PEO(5)/LiTFSI Sample Preparation. Poly(ethylene oxide) with molecular weight 5.0 kg mol^{-1} was obtained from Polymer Source, and LiTFSI was obtained from Novolyte. Both were dried under vacuum at 90 °C for 3 days in the glovebox antechamber. The polymer and salt were dissolved in THF and stirred at 45 °C for 1−2 h at the r values of interest. Following complete dissolution, the mixture was poured into a Teflon dish and allowed to dry on a hot plate at 45 °C overnight in the glovebox. Upon evaporating off the THF, the sample was then dried under vacuum at 90 °C overnight in a glovebox antechamber. Samples for electrochemical impedance testing were constructed as described in the corresponding section above, with the exception of the use of fiberglass fabric-reinforced silicone rubber spacers. These samples were approximately 800 μm in thickness.

■ RESULTS AND DISCUSSION

The SAXS profiles obtained at 25 °C after the heating and cooling cycle are shown in Figure 2, where the SAXS intensity, I, is plotted as a function of the magnitude of the scattering vector, q. For PEO—PSLiTFSI(5-2) a weak scattering maximum is observed at $q = q^* = 0.307$ nm^{-1}. For PEO—PSLiTFSI(5-3) and -(5-4), well-defined primary scattering peaks are observed at $q^* = 0.228$ and 0.226 nm^{-1}, respectively. These values correspond to domain spacings, d, the center-to-center distance between adjacent PEO-rich lamellae, of 20.4, 27.6, and 27.8 nm ($d = 2\pi/q^*$) for PEO—PSLiTFSI(5-2), -(5-3), and -(5-4), respectively. Higher order peaks in the vicinity of $2q^*$, $3q^*$, and $4q^*$ are observed for these three polymers as well. SAXS profiles of polymers with a higher content of PSLiTFSI, PEO—PSLiTFSI(5-5), -(5-7), and -(5-8) do not contain any peaks as shown in Figure 2a. It is evident that increasing the PSLiTFSI molecular weight from 4.0 to 5.4 kg mol^{-1} results in a change in the room temperature morphology from ordered to disordered. Also shown in Figure 2a are data obtained from PEO—PSLiTFSI(5-5) in the unannealed state
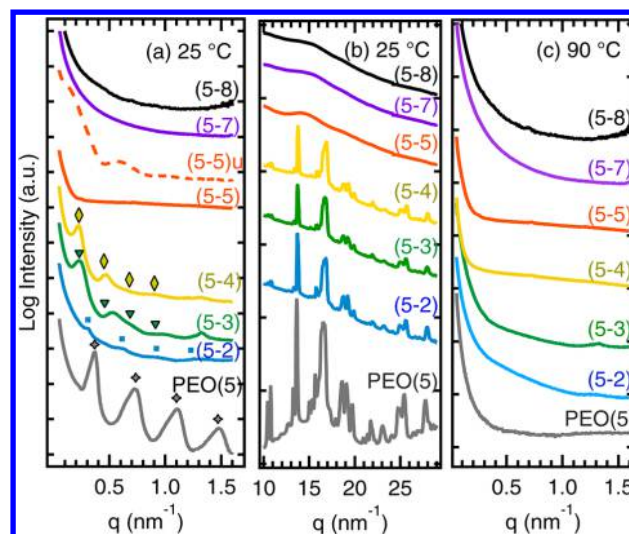

Figure 2. Scattering data shown are vertically offset for clarity. (a) SAXS intensity versus the magnitude of the scattering vector, q, at 25 °C of PEO-*b*-PSLiTFSI copolymers and PEO homopolymer. The markers shown, gray stars, blue rectangles, green triangles, and yellow diamonds, designate q^*, $2q^*$, $3q^*$, and $4q^*$ for ordered samples. Most of the data shown were obtained during the second heating run except for (5-5)u where the data were obtained from an unannealed sample during the first heating run. (b) WAXS intensity versus the magnitude scattering vector, q, at 25 °C of PEO-*b*-PSLiTFSI copolymers. (c) SAXS intensity versus magnitude of the scattering vector, q, at 90 °C of PEO-*b*-PSLiTFSI copolymers.

before commencing the heating and cooling cycle, labeled (5-5)u in Figure 2a. A weak scattering shoulder and a broad higher order scattering peak are evident in this sample. We thus conclude that PEO—PSLiTFSI(5-5) is at the border between order and disorder. The unannealed sample was held at room temperature for 9 days before the SAXS measurements were made. It is evident that weak order is obtained in the sample after extensive annealing at room temperature. In contrast, the cycled PEO—PSLiTFSI(5-5) sample shows no evidence of order (Figure 2a). In all other cases, the unannealed and cycled SAXS profiles obtained at room temperature were qualitatively similar. We conclude that order formation in PEO-*b*-PSLiTFSI is relatively rapid when the molecular weight of the PSLiTFSI block is ≤4.0 kg mol^{-1}. On the other hand, when the molecular weight of the PSLiTFSI block is ≥7.2 kg mol^{-1}, ordered phases are absent regardless of annealing time at room temperature.

The SAXS profile of homopolymer PEO(5) is also shown in Figure 2a. This profile is qualitatively similar to that obtained from the ordered block copolymers with a primary scattering peak at $q^* = 0.368$ nm^{-1} and higher order scattering peaks at $2q^*$, $3q^*$, and $4q^*$. Similar SAXS profiles of PEO have been reported in the literature.[24] The SAXS signal in semicrystalline polymers is due to contrast between crystalline and amorphous domains. The domain spacing of PEO(5), which represents the distance between adjacent PEO lamellar crystals, is 17.1 nm. Comparing the data obtained from PEO(5) to that obtained of PEO-*b*-PSLiTFSI (Figure 2), we conclude that order formation in the block copolymers is driven by the crystallization of PEO. It appears as if the PSLiTFSI block is accommodated within the amorphous phase. Increasing the length of the PSLiTFSI block results in an increase in d up to a maximum of 27.8 nm when the PSLiTFSI block molecular weight is 4.0 kg mol^{-1}. Further

increase of the PSLiTFSI block molecular weight results in a disordered morphology.

Wide-angle X-ray scattering profiles shown in Figure 2b confirm the crystalline nature of the block copolymers with PSLiTFSI block molecular weights ≤4.0 kg mol^{-1}. The scattering profile of PEO(5) is shown in gray for comparison. (The intensity of this profile was divided by a factor of 10 to facilitate comparison with the block copolymers.) Differential scanning calorimetry experiments reveal a melting temperature of 52 ± 4 °C for PEO−PSLiTFSI(5-2), -(5-3), and -(5-4), consistent with the scattering data (Figure S3).

The SAXS profiles of PEO−PSLiTFSI and the PEO homopolymer all have a low q upturn (Figure 2a). We attribute this to the lack of perfect periodic order and the presence of large length scale structures (e.g., spherulites) in both the homopolymer and the block copolymers. The locations of the observed higher order peaks in Figure 2a are not in perfect agreement with the expected locations for a lamellar phase. We attribute this to the complexity of order formation in the presence of crystallization.[25,26]

In Figure 2c, we show data obtained from the block copolymers at 90 °C, which is above the crystalline melting temperature of PEO(5). All of the samples are disordered at this temperature. The SAXS and WAXS profiles for samples PEO−PSLiTFSI(5-5), -(5-7), and -(5-8) are essentially independent of temperature. (See similarity of SAXS profiles obtained from these samples at 25 and 90 °C in Figures 2a and 2c.)

Samples PEO−PSLiTFSI(5-2), -(5-3), and -(5-4) exhibit a peak at $q \approx 1.3$ nm^{-1}, which we attribute to the presence of ionic clusters. SAXS in the vicinity of this peak for selected samples is shown in Figure 3. This peak is often referred to as
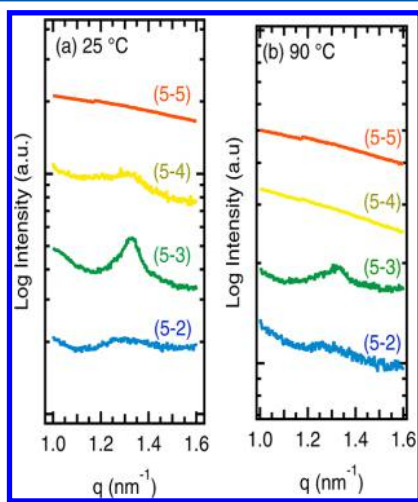

Figure 3. SAXS intensity versus the magnitude of the scattering vector, q, for PEO−PSLiTFSI(5-2), -(5-3), -(5-4), and -(5-5) in the vicinity of the ion cluster peak at (a) 25 and (b) 90 °C.

the ionomer peak, and it is found in numerous charged polymers.[27−30] This peak indicates that the ionic clusters are separated by a distance of about 5 nm ($2\pi/1.3$). The peak intensity is a nonmonotonic function of charge concentration. At 25 °C, PEO−PSLiTFSI(5-3) exhibits the highest cluster peak intensity (Figure 3a). Peaks with significantly lower intensity are seen in PEO−PSLiTFSI(5-2) and -(5-4) at 25 °C. The cluster peak is absent in PEO−PSLiTFSI(5-5) (Figure 3a) and in samples with higher PSLiTFSI volume fraction. It is

evident that at 25 °C the cluster peak is only seen in samples that are ordered. In all cases, the cluster peak intensity decreases with increasing temperature. At 90 °C, only the cluster peak in PEO−PSLiTFSI(5-3) is significantly above the background.

The temperature dependence of the ionic conductivity of the samples listed in Table 1 is shown in Figure 4. Samples that are
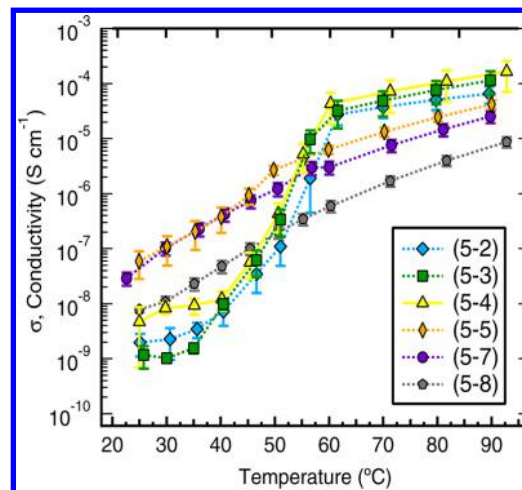

Figure 4. Ionic conductivity, σ, versus temperature of PEO-b-PSLiTFSI copolymers.

disordered over the entire temperature range, e.g., PEO−PSLiTFSI(5-8), exhibit relatively simple behavior that is consistent with the Vogel−Fulcher−Tammann−Hesse relationship that is often used to describe the ionic conductivity of homopolymer electrolytes.[3] In contrast, dramatic changes in the conductivity are observed in samples that exhibit an order-to-disorder transition, e.g., PEO−PSLiTFSI(5-3).

The dependence of conductivity on temperature and molecular structure (Figure 4) can be explained by using the morphological characterization described above. At low temperatures, the ionic groups in PEO−PSLiTFSI(5-2), -(5-3), and -(5-4) are sequestered in clusters in the PSLiTFSI microphase, and the crystalline PEO microphases are devoid of ions. Both factors contribute to conductivities between 10^{-9} and 10^{-8} S cm^{-1} in the ordered state at temperatures below the PEO microphase melting temperature. These same polymers exhibit high conductivities in the disordered state above 60 °C. The conductivities of the ordered samples increase abruptly, by as much as 5 orders of magnitude, across the order-to-disorder transition. No abrupt changes in conductivity are seen in samples that are fully disordered—PEO−PSLiTFSI(5-5), -(5-7), and -(5-8); see Figure 4.

Increasing the molecular weight of the PSLiTFSI block increases ion concentration. This however has a nontrivial effect on ionic conductivity because the volume fraction of the ion-conducting PEO domains decreases with increasing ion concentration (see Table 1). This interplay is clarified in Figure 5 where conductivity is plotted as a function of Li$^+$ concentration, r, at selected temperatures. At 45 °C, conductivity generally increases with increasing salt concentration up to $r = 0.199$ before decreasing abruptly in the $r = 0.207$ sample. It is perhaps interesting to note that this abrupt decrease in conductivity of PEO−PSLiTFSI(5-8), the polymer with the highest ion concentration, is seen at all temperatures (Figure 5). At 55 °C, ionic conductivity is a weak decreasing
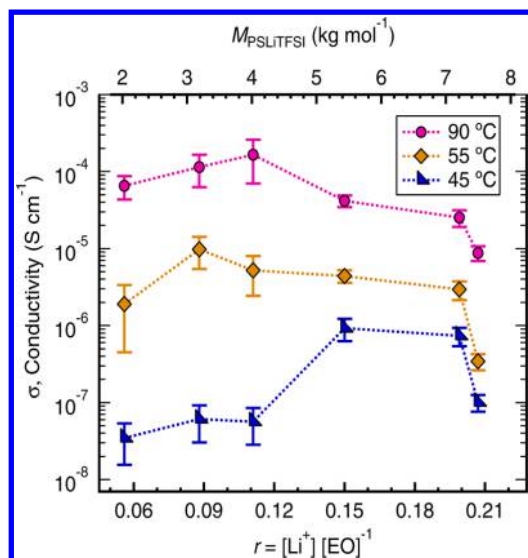
Figure 5. Ionic conductivity, σ, versus salt concentration (r) for temperatures 45, 55, and 90 °C. The top axis identifies the molecular weight of the PSLiTFSI block.

PSLiTFSI domains. We propose that this is due to two effects: favorable interactions between Li^+ and PEO and the entropy of Li^+ counterions. Complexation of Li^+ by PEO chains is well-established,[31] and disordering enables contact between Li^+, that are nominally located on the PSLiTFSI block, and PEO segments. Figure 5 shows a dramatic increase in low-temperature conductivity when r is increased from 0.111 to 0.150, which is a clear indication of the presence of free Li^+ counterions. As the molecular weight of the PSLiTFSI block increases, the concentration of ions increases as well, increasing the importance of Li^+ counterion entropy.[32] Beyond a critical charge concentration, $r > 0.111$, in the present set of samples, favorable energetic interactions between the Li^+ and PEO segments and contributions to the free energy of the block copolymer due to counterion entropy increase and overwhelm the forces that drive PEO crystallization at room temperature.

To shed light on the complex interplay between conductivity and molecular structure, we define a normalized conductivity, σ_n:

$$\sigma_n(T) = \frac{\sigma(T)}{\sigma_{PEO}(T)\phi_{PEO}} \tag{1}$$

function of r over most of the experimental window from r = 0.088 to 0.207. At 90 °C, conductivity increases with increasing ion concentration up to r = 0.111, and then it decreases at higher ion concentration. The ratio σ/r at 90 °C is nearly constant in the low concentration regime; at r = 0.056, 0.088, and 0.111, $\sigma/r = (1.32 \pm 0.17) \times 10^{-3}$ S cm^{-1}. We thus attribute the conductivity increase at low r values (90 °C) to an increase in ion concentration. Effects other than ion concentration dominate the behavior of these block copolymer electrolytes at other temperatures and r values.

Returning to Figure 2, we can now address the underlying reason for disappearance of crystallinity at room temperature when the molecular weight of the PSLiTFSI exceeds 4.0 kg mol^{-1} while the PEO molecular weight is constant at 5.0 kg mol^{-1}. The fact that both crystallinity and microphase separation disappear at the same ion concentration indicates that the two phenomena are coupled. In other words, PEO crystallinity is lost when Li^+ ions are not confined to the

where σ_{PEO} is the conductivity of PEO(5)/LiTFSI mixtures (5.0 kg mol^{-1} PEO homopolymer) at the r value of interest. We restrict our attention to temperatures between 60 and 90 °C where all the polymers are disordered. In Figure 6a, we plot σ_{PEO} versus r for temperatures 60–90 °C. We used this data set to calculate normalized conductivities, and the results are shown in Figure 6b, where σ_n is plotted as a function of r. The data at the different temperatures collapse on one another, with an average difference of about 15% between values at each temperature. The relatively large error bars in Figure 6b are due to the limited number of samples that we could examine and the fact that the samples were difficult to handle. The normalized conductivity, σ_n, is peaked at r = 0.111. The conductivity maximum in PEO(5)/LiTFSI is also obtained at r = 0.111 (Figure 6a). This value is similar to that reported for PEO/LiTFSI mixtures.[33]

Equation 1 does not account for the fact that the Li^+ transference number, t^+, in PEO homopolymer and PEO-*b*-
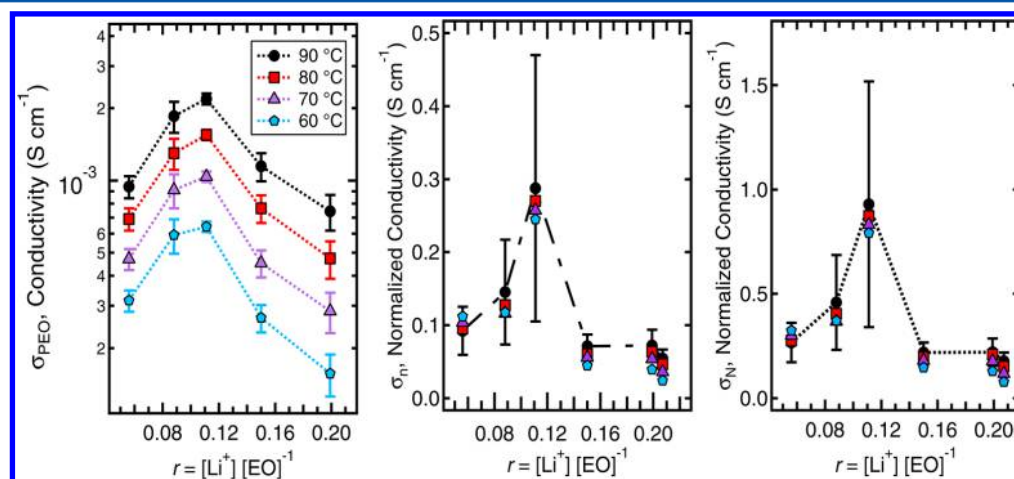

Figure 6. (a) Ionic conductivity of PEO(5)/LiTFSI, σ_{PEO}, versus salt concentration (r) for temperatures 60−90 °C. (b) Normalized ionic conductivity of PEO-*b*-PSLiTFSI copolymers, σ_n, as defined by eq 1, versus r, for temperatures 60−90 °C. The data at these different temperatures roughly collapse on one another. (c) Normalized ionic conductivity of PEO-*b*-PSLiTFSI copolymers corrected for transference number, σ_N, as defined by eq 2, versus r, for temperatures 60−90 °C. The data at these different temperatures are within close proximity to one another.

PSLiTFSI block copolymers are very different. The steady-state-current method was used to estimate t^+ of the PEO-b-PSLiTFSI samples, and the results are tabulated in Table 1. This method is only accurate when t^+ is close to unity as effects due to the friction between oppositely charged ions and nonideality of mixing are not accounted.[4,21,34] The values of t^+ obtained for PEO-b-PSLiTFSI samples ranged from 0.87 to 0.99. In our analysis, we assume $t^+_{PEO} = 0.30$, for the PEO(5)/LiTFSI mixtures, independent of salt concentration.[35] Literature values for t^+_{PEO} range between 0.10 and 0.50.[36−40] It is conceivable that t^+ in polymer/salt mixtures decreases with increasing salt concentration due to ion complexation,[41] but this effect has not yet been quantified for PEO/LiTFSI. We also assume that the transference number in both these systems is independent of temperature. We define a transference-number-corrected normalized conductivity, σ_N:

$$\sigma_N(T) = \frac{\sigma(T)t^+}{\sigma_{PEO}(T)\phi_{PEO}t^+_{PEO}} \tag{2}$$

where t^+ is the lithium ion transference number reported in Table 1. In Figure 6c, we plot σ_N versus r. The normalized conductivity, σ_N, approaches unity at $r = 0.111$. It is evident that PEO−PSLiTFSI(5-4) is the most effective single-ion-conducting block copolymer electrolyte that we have studied thus far. The maximum conductivity of this copolymer is 1.65×10^{-4} S cm^{-1} at 90 °C.

Our analysis suggests that in the highly conducting electrolytes $\sigma/r = 1.32 \times 10^{-3}$ S cm^{-1} at 90 °C. Using this relationship, we estimate a conductivity of 3.70×10^{-5} S cm^{-1} at $r = 0.028$. In their study of PSLiTFSI-b-PEO-b-PSLiTFSI, Bouchet et al. determined that the most conductive electrolyte in their sample set had $r = 0.028$, and their reported conductivity of 3.4×10^{-5} S cm^{-1} at 90 °C is in agreement with the proposed relationship.

CONCLUSION

We have synthesized and characterized a series of single-ion-conducting block copolymer electrolytes, PEO-b-PSLiTFSI, where the PEO molecular weight was held fixed at 5.0 kg mol^{-1}, and the ion-containing block, PSLiTFSI, was varied from 2.0 to 7.5 kg mol^{-1}. Below the PEO melting temperature (52 ± 4 °C), a lamellar morphology with ion clusters were found for PEO−PSLiTFSI(5-2), -(5-3), and -(5-4). These polymers exhibited an order-to-disorder transition coincident with the melting of the PEO crystals, and the conductivity increased abruptly by as much as 5 orders of magnitude. Polymers with higher Li$^+$ content, PEO−PSLiTFSI(5-7) and -(5-8), were disordered at all temperatures, and their conductivities were a smooth function of temperature. PEO−PSLiTFSI(5-5) was shown to lie at the border between partially ordered and fully disordered systems. Samples that exhibited conductivities above 10^{-5} S cm^{-1} were all disordered. However, samples that exhibited the highest conductivities at high temperatures were ordered at low temperatures (see Figures 4 and 5). In contrast, samples that exhibited low conductivities in the high-temperature disordered state were also disordered at low temperatures. Ion transport in PEO-b-PSLiTFSI copolymers depends on a complex interplay between the volume fraction of the PEO block that provides avenues for ion transport and that of the PSLiTFSI block where the ions are stored.

ASSOCIATED CONTENT

ⓢ Supporting Information

The Supporting Information is available free of charge on the ACS Publications website at DOI: 10.1021/acs.macromol.5b01193.

> GPC traces of the PEO-b-PSLiTFSI copolymers; details on the conductivity sample construction; DSC thermograms and thermodynamic data for PEO-b-PSLiTFSI; transference number measurement details (PDF)

AUTHOR INFORMATION

Corresponding Author

*E-mail nbalsara@berkeley.edu, Ph (510) 642-8937 (N.P.B.).

Author Contributions

A.A.R. and S.I. made equal contributions.

Notes

The authors declare no competing financial interest.

NOMENCLATURE

Abbreviations

LiTFSI	lithium bis(trifluoromethane sulfonyl)imide
PEO	poly(ethylene oxide)
PEO-b-PSLiTFSI	poly(ethylene oxide)-b-polystyrenesulfonyl-lithium (trifluoromethylsulfonyl)imide
PS	polystyrene
SAXS	small-angle X-ray scattering
THF	tetrahydrofuran
WAXS	wide-angle X-ray scattering

Symbols

d	the domain spacing
$Đ$	the dispersity
M_{PEO}	molecular weight of the PEO block
$M_{PSLiTFSI}$	molecular weight of the PSLiTFSI block
t^+	the lithium ion transference number
t^+_{PEO}	transference number of PEO/LiTFSI system

Greeks

$\sigma_{PEO}(T)$	ionic conductivity of PEO/LiTFSI system
$\sigma_n(T)$	normalized conductivity
$\sigma_N(T)$	transference number corrected normalized conductivity
$\sigma(T)$	ionic conductivity
ϕ_{PEO}	volume fraction of the PEO block

■ REFERENCES

(1) Monroe, C.; Newman, J. The Impact of Elastic Deformation on Deposition Kinetics at Lithium/Polymer Interfaces. *J. Electrochem. Soc.* **2005**, *152*, A396.

(2) Singh, M.; Odusanya, O.; Wilmes, G. M.; Eitouni, H. B.; Gomez, E. D.; Patel, A. J.; Chen, V. L.; Park, M. J.; Fragouli, P.; Iatrou, H.; Hadjichristidis, N.; Cookson, D.; Balsara, N. P. Effect of Molecular Weight on the Mechanical and Electrical Properties of Block Copolymer Electrolytes. *Macromolecules* **2007**, *40*, 4578−4585.

(3) Young, W.-S.; Kuan, W.-F.; Epps, T. H. Block Copolymer Electrolytes for Rechargeable Lithium Batteries. *J. Polym. Sci., Part B: Polym. Phys.* **2014**, *52*, 1−16.

(4) Newman, J.; Thomas-Alyea, K. E. *Electrochemical Systems*, 3rd ed.; John Wiley & Sons, Inc.: Hoboken, NJ, 2004.

(5) Monroe, C.; Newman, J. Dendrite Growth in Lithium/Polymer Systems. *J. Electrochem. Soc.* **2003**, *150*, 150.

(6) Bartels, J.; Hess, A.; Shiau, H.-S.; Allcock, H. R.; Colby, R. H.; Runt, J. Synthesis, Morphology, and Ion Conduction of Polyphosphazene Ammonium Iodide Ionomers. *Macromolecules* **2015**, *48*, 111−118.

(7) Bouchet, R.; Maria, S.; Meziane, R.; Aboulaich, A.; Lienafa, L.; Bonnet, J.-P.; Phan, T. N. T.; Bertin, D.; Gigmes, D.; Devaux, D.; Denoyel, R.; Armand, M. Single-Ion BAB Triblock Copolymers as Highly Efficient Electrolytes for Lithium-Metal Batteries. *Nat. Mater.* **2013**, *12*, 452−457.

(8) Gomez, E. D.; Panday, A.; Feng, E. H.; Chen, V.; Stone, G. M.; Minor, A. M.; Kisielowski, C.; Downing, K. H.; Borodin, O.; Smith, G. D.; Balsara, N. P. Effect of Ion Distribution on Conductivity of Block Copolymer Electrolytes. *Nano Lett.* **2009**, *9*, 1212−1216.

(9) Bates, F. S.; Fredrickson, G. H. Block Copolymer Thermodynamics: Theory and Experiment. *Annu. Rev. Phys. Chem.* **1990**, *41*, 525−57.

(10) Sing, C. E.; Zwanikken, J. W.; Olvera de la Cruz, M. Electrostatic Control of Block Copolymer Morphology. *Nat. Mater.* **2014**, *13*, 694−698.

(11) Teran.; et al. Discontinuous Changes in Ionic Conductivity of a Block Copolymer Electrolyte through an Order-Disorder Transition. *ACS Macro Lett.* **2012**, *1*, 305−309.

(12) Cheng, S.; Smith, D. M.; Li, C. Y. How Does Nanoscale Crystalline Structure Affect Ion Transport in Solid Polymer Electrolytes? *Macromolecules* **2014**, *47*, 3978−3986.

(13) Young, N. P.; Devaux, D.; Khurana, R.; Coates, G. W.; Balsara, N. P. Investigating Polypropylene-Poly(Ethylene Oxide)-Polypropylene Triblock Copolymers as Solid Polymer Electrolytes for Lithium Batteries. *Solid State Ionics* **2014**, *263*, 87−94.

(14) Ryu, S.-W.; Trapa, P. E.; Olugebefola, S. C.; Gonzalez-Leon, J. A.; Sadoway, D. R.; Mayes, A. M. Effect of Counter Ion Placement on Conductivity in Single-Ion Conducting Block Copolymer Electrolytes. *J. Electrochem. Soc.* **2005**, *152*, A158.

(15) Choi, U. H.; Ye, Y.; Salas de la Cruz, D.; Liu, W.; Winey, K. I.; Elabd, Y. A.; Runt, J.; Colby, R. H. Dielectric and Viscoelastic Responses of Imidazolium-Based Ionomers with Different Counterions and Side Chain Lengths. *Macromolecules* **2014**, *47*, 777−790.

(16) Kuan, W.-F.; Remy, R.; Mackay, M. E.; Epps, T. H. Controlled Ionic Conductivity via Tapered Block Polymer Electrolytes. *RSC Adv.* **2015**, *5*, 12597−12604.

(17) Inceoglu, S.; Rojas, A. A.; Devaux, D.; Chen, X. C.; Stone, G. M.; Balsara, N. P. Morphology-Conductivity Relationship of Single-Ion-Conducting Block Copolymer Electrolytes for Lithium Batteries. *ACS Macro Lett.* **2014**, *3*, 510−514.

(18) Wanakule, N. S.; Panday, A.; Mullin, S. A.; Gann, E.; Hexemer, A.; Balsara, N. P. Ionic Conductivity of Block Copolymer Electrolytes in the Vicinity of Order−Disorder and Order−Order Transitions. *Macromolecules* **2009**, *42*, 5642−5651.

(19) van Krevelen, D. W. *Properties of Polymers: Their Correlation with Chemical Structure, Their Numerical Estimation and Prediction from Additive Group Contributions*, 4th ed.; Elsevier: Amsterdam, 2009.

(20) Bruce, P. G.; Vincent, C. A. Steady State Current Flow in Solid Binary Electrolyte Cells. *J. Electroanal. Chem. Interfacial Electrochem.* **1987**, *225*, 1−17.

(21) Doyle, M. Analysis of Transference Number Measurements Based on the Potentiostatic Polarization of Solid Polymer Electrolytes. *J. Electrochem. Soc.* **1995**, *142*, 3465.

(22) Hexemer, A.; Bras, W.; Glossinger, J.; Schaible, E.; Gann, E.; Kirian, R.; Macdowell, A.; Church, M.; Rude, B.; Padmore, H. A SAXS/WAXS/GISAXS Beamline With Multilayer Monochromator. *J. Phys.: Conf. Ser.* **2010**, *247*, 012007.

(23) Ilavsky, J. Nika: Software for Two-Dimensional Data Reduction. *J. Appl. Crystallogr.* **2012**, *45*, 324−328.

(24) Wang, W.; Liu, W.; Tudryn, G. J.; Colby, R. H.; Winey, K. I. Multi-Length Scale Morphology of Poly(Ethylene Oxide)-Based Sulfonate Ionomers with Alkali Cations at Room Temperature. *Macromolecules* **2010**, *43*, 4223−4229.

(25) Loo, Y.-L.; Register, R. A.; Ryan, A. J. Modes of Crystallization in Block Copolymer Microdomains: Breakout, Templated, and Confined. *Macromolecules* **2002**, *35*, 2365−2374.

(26) Rangarajan, P.; Register, R. A.; Fetters, L. J. Morphology of Semicrystalline Block Copolymers of Ethylene-(Ethylene-Alt-Propylene). *Macromolecules* **1993**, *26*, 4640−4645.

(27) Beers, K. M.; Balsara, N. P. Design of Cluster-free Polymer Electrolyte Membranes and Implications on Proton Conductivity. *ACS Macro Lett.* **2012**, *1*, 1155−1160.

(28) Yarusso, D. J.; Cooper, S. L. Microstructure of Ionomers: Interpretation of Small-Angle X-Ray Scattering Data. *Macromolecules* **1983**, *16*, 1871−1880.

(29) Hsu, W. Y.; Gierke, T. D. Ion Transport and Clustering in Nafion Perfluorinated Membranes. *J. Membr. Sci.* **1983**, *13*, 307−326.

(30) Lee, D.; Register, R. A.; Yang, C.; Cooper, S. L. MDI-Based Polyurethane Ionomers. 1. New Small-Angle X-Ray Scattering Model. *Macromolecules* **1988**, *21*, 998−1004.

(31) Mao, G.; Saboungi, M.-L.; Price, D. L.; Armand, M. B.; Howells, W. S. Structure Of Liquid PEO-LiTFSI Electrolyte. *Phys. Rev. Lett.* **2000**, *84*, 5536−5539.

(32) Marko, J. F.; Rabin, Y. Microphase Separation of Charged Diblock Copolymers: Melts and Solutions. *Macromolecules* **1992**, *25*, 1503−1509.

(33) Lascaud, S.; Perrier, M.; Vallee, A.; Besner, S.; Prud'homme, J.; Armand, M. Phase Diagrams And Conductivity Behavior of Poly-(Ethylene Oxide)-Molten Salt Rubbery Electrolytes. *Macromolecules* **1994**, *27*, 7469−7477.

(34) Doyle, M.; Fuller, T. F.; Newman, J. The Importance of the Lithium Ion Transference Number in Lithium/Polymer Cells. *Electrochim. Acta* **1994**, *39*, 2073−2081.

(35) Timachova, K. Personal communication.

(36) Ghosh, A.; Wang, C.; Kofinas, P. Block Copolymer Solid Battery Electrolyte with High Li-Ion Transference Number. *J. Electrochem. Soc.* **2010**, *157*, A846.

(37) Capuano, F. Composite Polymer Electrolytes. *J. Electrochem. Soc.* **1991**, *138*, 1918.

(38) Appetecchi, G. B.; Zane, D.; Scrosati, B. PEO-Based Electrolyte Membranes Based on $LiBC_4O_8$ Salt. *J. Electrochem. Soc.* **2004**, *151*, A1369.

(39) Evans, J.; Vincent, C. A.; Bruce, P. G. Electrochemical Measurement of Transference Numbers in Polymer Electrolytes. *Polymer* **1987**, *28*, 2324−2328.

(40) Watanabe, M. Effects of Network Structures and Incorporated Salt Species on Electrochemical Properties of Polyether-Based Polymer Electrolytes. *Solid State Ionics* **1995**, *79*, 306−312.

(41) Thomas, K. E.; Sloop, S. E.; Kerr, J. B.; Newman, J. Comparison of Lithium-Polymer Cell Performance with Unity and Nonunity Transference Numbers. *J. Power Sources* **2000**, *89*, 132−138.